JPRS 77528

6 March 1981

China Report

SCIENCE AND TECHNOLOGY

No. 85

FBIS FOREIGN BROADCAST INFORMATION SERVICE

NOTE

JPRS publications contain information primarily from foreign newspapers, periodicals and books, but also from news agency transmissions and broadcasts. Materials from foreign-language sources are translated; those from English-language sources are transcribed or reprinted, with the original phrasing and other characteristics retained.

Headlines, editorial reports, and material enclosed in brackets [] are supplied by JPRS. Processing indicators such as [Text] or [Excerpt] in the first line of each item, or following the last line of a brief, indicate how the original information was processed. Where no processing indicator is given, the information was summarized or extracted.

Unfamiliar names rendered phonetically or transliterated are enclosed in parentheses. Words or names preceded by a question mark and enclosed in parentheses were not clear in the original but have been supplied as appropriate in context. Other unattributed parenthetical notes within the body of an item originate with the source. Times within items are as given by source.

The contents of this publication in no way represent the policies, views or attitudes of the U.S. Government.

PROCUREMENT OF PUBLICATIONS

JPRS publications may be ordered from the National Technical Information Service, Springfield, Virginia 22161. In ordering, it is recommended that the JPRS number, title, date and author, if applicable, of publication be cited.

Current JPRS publications are announced in Government Reports Announcements issued semi-monthly by the National Technical Information Service, and are listed in the Monthly Catalog of U.S. Government Publications issued by the Superintendent of Documents, U.S. Government Printing Office, Washington, D.C. 20402.

Indexes to this report (by keyword, author, personal names, title and series) are available from Bell & Howell, Old Mansfield Road, Wooster, Ohio 44691.

Correspondence pertaining to matters other than procurement may be addressed to Joint Publications Research Service, 1000 North Glebe Road, Arlington, Virginia 22201.

JPRS 77526

6 March 1981

CHINA REPORT

SCIENCE AND TECHNOLOGY

No. 85

CONTENTS

ABSTRACTS

APPLIED SCIENCES

NATION'S FIRST LARGE, HIGH-FLUX REACTOR UNVEILED

Hong Kong TA KUNG PAO in China 12 Feb 81 p 1

[Photograph captions]

[Text] The first large, high-flux nuclear reactor designed and built by the Chinese themselves was recently completed in southwestern China and went into high power operation. The construction of this reactor demonstrates that China now has the ability to independently design and build nuclear power stations.

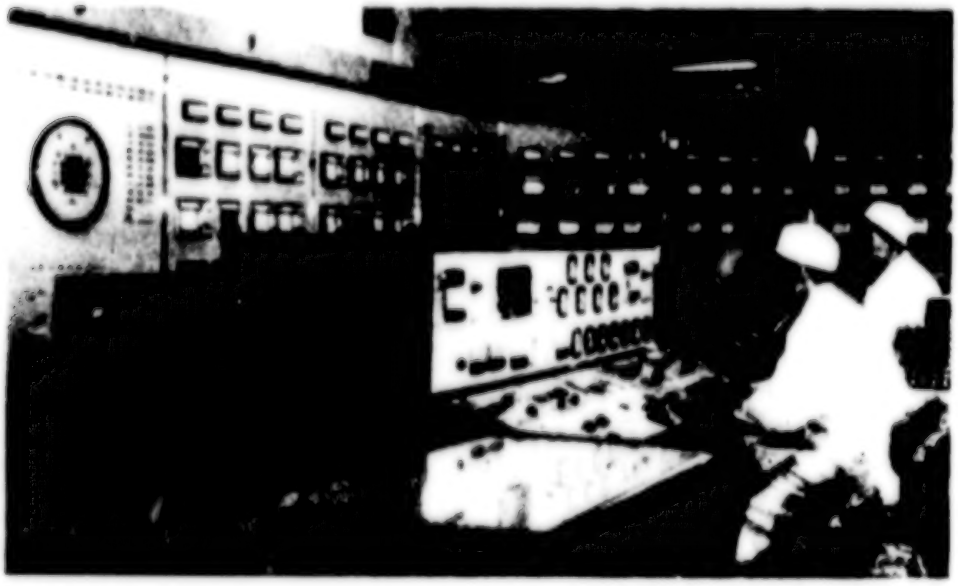

Workers in the main control room monitor the operation of the reactor.

Technicians engaged in preparatory work.

CSO: 4008

HIGH-PRECISION REMOTE SENSING RESEARCH DESCRIBED

Shanghai DIANZI JISHU in Chinese No 9, 1980 pp 1-6

[Article by Su Jiexuan [5685 2638 6513]: "High-Precision Remote Sensing Research"]

[Text] There are cases when it is required to measure certain parameters of moving bodies, for example the deformation of turbine blades rotating at high speed, changes in the properties of various components of a new motor vehicle during testing, changes in tire pressure and temperature at various points during simulated highway testing, and the like. During the measurement, there are certain difficulties in directly extracting a signal which reflects the changes in the relevant parameters. Sometimes the signal can of course be directly led out by using a slip ring, but at present there are still some difficulties in producing high-quality slip rings. In addition, if the object on which measurements are being taken is too far from the control center, a long-distance lead wire is both inconvenient and sometimes is impossible. Accordingly, it is especially necessary to develop high-precision, small-size, lightweight radio transmitters to solve the difficulties described above in practice.

During its investigation of the motion characteristics of automobile tires, a certain organization in Beijing requested that we help it solve problems of measuring the internal pressure (0-10 kg/cm^2) of tires rotating at high speed on a test machine. They requested that the remote sensing accuracy be to 1 to 2 decimal places, that the device operate continuously for 4 hours, and that it be designed around the BPR-2 pressure sensor.

1. Problem Approach

In the past, the amplitude modulation [AM] and frequency modulation [FM] approaches were frequently adopted in remote sensing equipment, and in recent years the AM-FM method has been used both in this country and abroad, but the accuracy of these methods is not high. The reason that the precision of AM type remote sensing equipment is not high is that when a wave amplitude modulated in proportion to the parameters being measured propagates in space, it may be affected by spatial state changes; various interference sources that may be present may also distort the amplitude-modulated signal. The equipment in question uses an on-site DC electric motor with large capacity controlled

by an SCR and other electrical equipment. Because of this poor environment, interference is a major problem and this method cannot assure high precision. Although the FM method can increase noise immunity, because the frequency-modulating components are highly nonlinear, and the linearity of a simple detector circuit is also not high, the precision of an FM type of remote sensing equipment can scarcely reach 5 percent.

On the basis of the above analysis, in order to further improve precision we need to find a new approach. The new approach which we devised was to convert changes in the parameters being measured into changes in pulse duration and then use these pulses to control a high-frequency oscillator which transmits them. The receiver restores the pulses and in addition converts the pulse duration changes into changes in an output voltage level, ultimately accomplishing the task of remote measurement of the relevant parameters. But during our research we found that if we only converted changes in the measured parameter into a change in pulse length, the receiver apparatus would be rather complex. If we can maintain the pulse rate constant so that the changes in the measured parameter become changes in the pulse duty factor, the receiver can be much simpler, because changes in the pulse duty factor reflect changes in an average value, and designing a circuit which reflects changes in an average value is very simple. At the same time, this method makes it possible for the equipment to have excellent noise immunity. On the basis of this conception, we converted the measured parameter into an electrical voltage, then had a comparator compare it with a fixed frequency sawtooth wave, obtaining a pulse output in which the pulse duty factor was proportional to the measured parameter; this was used to control the emissions of a fixed-frequency high frequency carrier. When the receiver receives this kind of electromagnetic wave, it converts it to a voltage output proportional to the measured parameter. This method is called Pulse Length Modulation (PLM). After more than a year's research and testing, we finally developed a high-precision, noise-immune remote sensing device. A block diagram and a circuit diagram are given in Figures 1 and 2.

2. Operating Principles

It can be seen from Figures 1 and 2 that after the measured signal is amplified, it is compared with a stable frequency sawtooth wave in comparator 2, which outputs pulses whose duty factor is proportional to the measured parameter. These pulses control transmission of a high-frequency wave via switching transistor BG3: when comparator 2 outputs a high voltage level, emission ceases, and in the reverse case emission proceeds. As a result, emission and interruption of the carrier wave correspond to the states of comparator 2 and thus to the input parameter that is being measured. A superheterodyne receiver receives this intermittent signal, and after detection obtains a square wave in which the duty factor corresponds to the output of comparator 2. A discriminator yields a constant-stable-amplitude square wave corresponding to the output state point of discriminator 2, and this signal controls switching transistor BG9 of the demodulator. When the discriminator output is a high voltage level, switching transistor BG9 is on and transistor BG10's emitter passes a constant current equal to E_W/R_{43}. When the discriminator output is a low voltage level, switching transistor BG9 is off, and the emitter of transistor BG10 passes zero current.

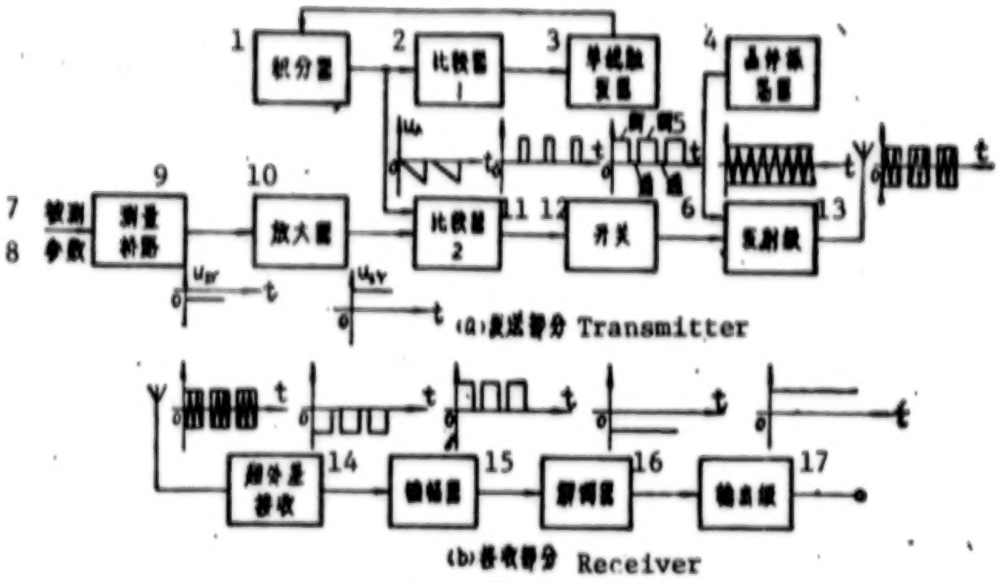

Figure 1.

Key:

1. Integrator
2. Comparator 1
3. Monostable multivibrator
4. Crystal oscillator
5. Off
6. On
7. Measured parameter
9. Measuring bridge circuit
10. Amplifier
11. Comparator 2
12. Switch
13. Transmitter stage
14. Superheterodyne receiver
15. Discriminator
16. Demodulator
17. Output stage

After filtering, a direct current voltage proportional to the measured parameter is obtained across R_{46}. The output stage produces a 0-100 mV DC potential corresponding to a gas pressure variation between 1 and 10 kg/cm^2. This effects remote sensing of the parameter to be measured, the pressure. It can be proved that the following excellent linear relationship holds between the received output u_{sc} and the measured pressure P:

$$u_{sc} = \frac{E_W - (V_{Be} + V_{ces})}{R_{43}} \cdot \frac{T_4 R_{28}}{E_s\left(\frac{R_6}{R_5} T_4 + \tau_k\right) R_{27}} \alpha\beta k_1 P \qquad (1)$$

where E_W is the fixed voltage of voltage stabilizer DW_3; V_{Be} is the voltage drop at the B-E junction of transistor BG10; V_{ces} is the saturation voltage drop across transistor BG9; τ_k is the quasistable state duration of the monostable multivibrator; τ_4 is the integral time constant ($=R_2C_1$); α is the ratio of the unbalanced voltage across the measurement bridge circuit to the pressure being measured; and β and k_1 are the gains of the amplifier and output stage.

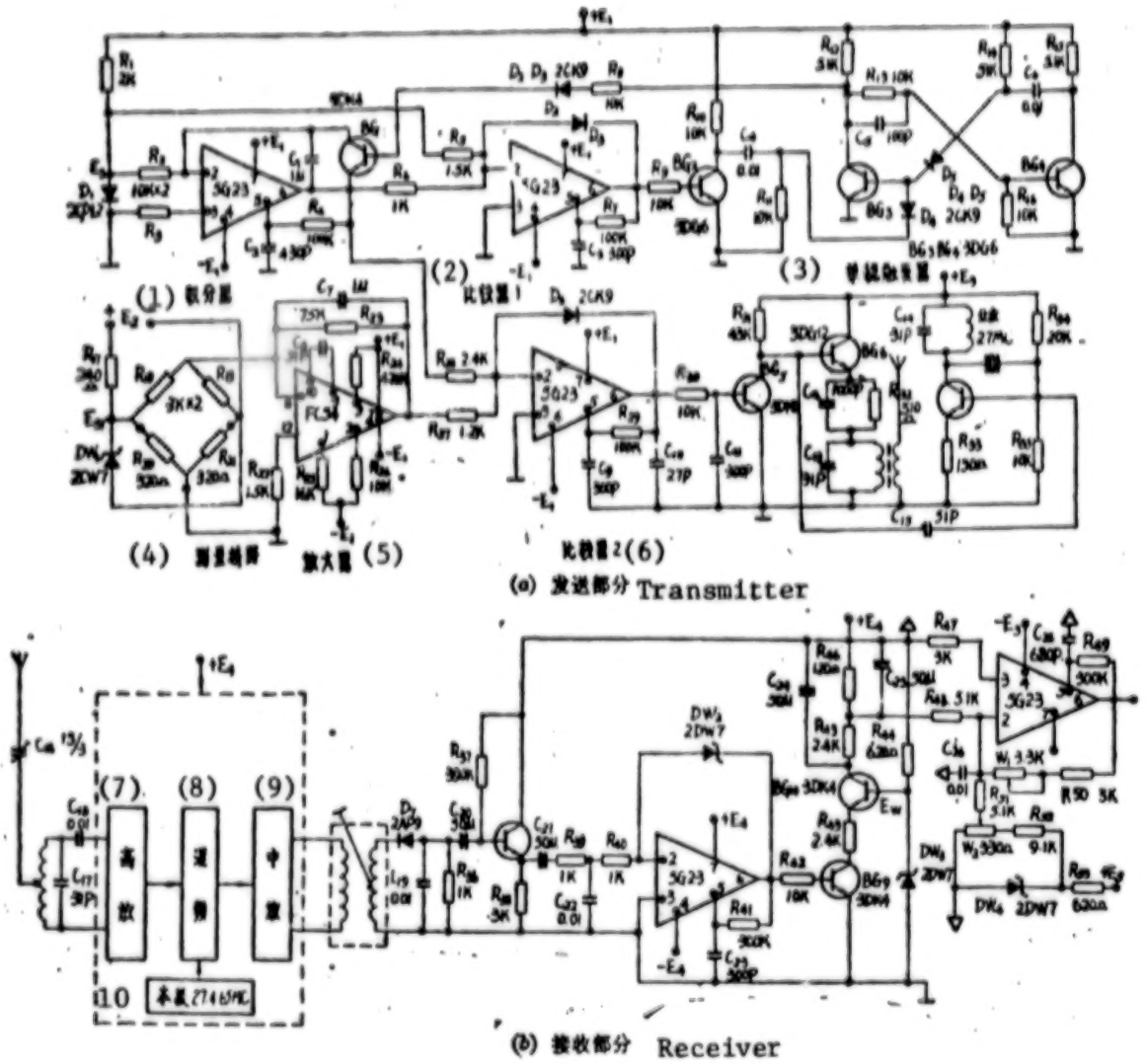

Figure 2.

Key:

1. Integrator
2. Comparator 1
3. Monostable multivibrator
4. Measuring bridge
5. Amplifier
6. Comparator 2
7. High-frequency amplifier
8. Mixer
9. Medium-frequency amplifier
10. Main oscillator

3. Several of the Principle Factors Affecting the Precision of the Apparatus

Because the sawtooth wave generator is composed of a relatively ideal integrator, comparator 1 and a monostable multivibrator, the linearity of the sawtooth wave is excellent, and the linearity of the device as a whole is also very good. Accordingly, the precision of the device is determined by the frequency

stability of the sawtooth wave, its rise speed, the stability of the ratio between the amplifier output voltage and the measured parameter (i.e. the stability of the relationship between the measured parameter and the pulse duty factor), the temperature stability and the quality of the noise immunity.

Because the transmitter is installed on an axle rotating at high speed, it cannot be directly fed by a stable power supply, which indeed is not permissible on-site, so that a battery must be used. Although a small, light, 5-unit nickel cadmium cell power supply with excellent qualities (each unit 1.25 volts, permissible continuous discharge current 22.5 mA, 10 hours continuous operation, stop voltage 1 V, weight 13 grams) is used, and in addition everything is done to assure low losses in the circuit, in continuous operation lasting more than 4 hours the power supply voltage will inevitably change. When designing the circuit we were aware of the effects on accuracy of the unit resulting from power supply voltage changes, and accordingly we devised a method of avoiding the effect.

Below we discuss several problems which affect the characteristics of the device.

A. Stability of the sawtooth wave frequency.

The constant frequency sawtooth wave generator circuit is shown in Figure 3.

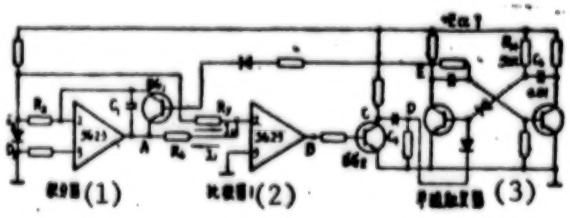

Figure 3.

Key: 1. Integrator 2. Comparator 1 3. Monostable multivibrator

If initially the integrator output is zero, under the influence of I_2 comparator 1 will produce a low output at B, and a high level output at C. When capacitor C4 finishes charging, the voltage at point D will be zero, and that at E will be low. Switching transistor BG1 will be open. Then, when the integrator begins to integrate, I_1 will gradually increase. When $|I_1| \geqslant |I_2|$, i.e. when $|u_A/R_6| \geqslant |e_S/R_5|$, the comparator will change state, B will go high, transistor BG2 will be saturated, a negative pulse will appear at D, and the monostable multivibrator will fire, the voltage will be high at E, switching transistor BG1 will turn on, integrating capacitor C_1 will discharge, and during the time τ_k when the monostable vibrator is in the quasistable state the electrical charge stored in integrating capacitor C_1 will rapidly be fully discharged and the integrator output will be zero. After a time much shorter than τ_k, comparator 1 will return to its initial state, the voltage at B will be low, the voltage at C will be high,

and capacitor C_4 will charge, preparing for the next firing. When the quasistable state of the multivibrator ends, switching transistor BG1 will turn off, integration will begin, and the process described above will be repeated. Accordingly the output u_A of the integrator will be a series of sawtooth waves. The waveforms at points A, B, C, D and E of Figure 3 are shown in Figure 4.

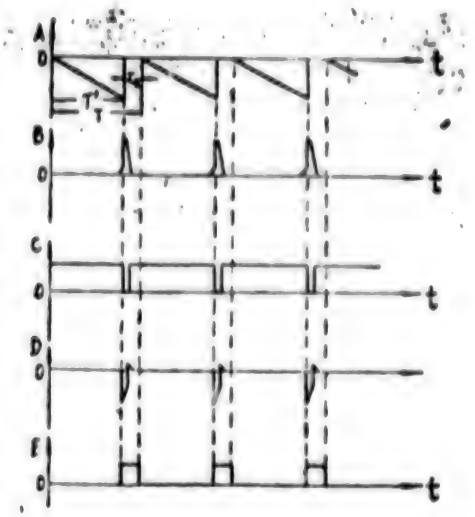

Figure 4.

It is clear from the foregoing analysis that when the gain of the amplifier consisting of the integrator and comparator 1 is great enough, the relationships given below can be used to determine the frequency of the sawtooth wave.

Because:

$$u_A(t) \approx \frac{1}{R_2C_1} \int_0^t E_s dt = \frac{E_s}{T_4} t; \qquad (2)$$

where E_s is the integrator input voltage and the reference voltage for comparator 1 and T_4 is the integrator time constant ($=R_2C_1$),.

When $t = T'$, $u_A(T') = E_s R_6/R_5$, comparator 1 reverses state, and integration concludes, so that

$$\frac{E_s}{T_4} T' = \frac{R_6}{R_5} E_s, \quad T' = \frac{R_6}{R_5} T_4' \qquad (3)$$

and accordingly the sawtooth wave period is

$$T = T' + \tau_k = \frac{R_6}{R_5} T_4 + \tau_k; \qquad (4)$$

When the battery voltage changes, although there may be a change in E_s, it is evident from equation (3) that T' is independent of E_s, and thus of the power supply voltage; this is because the integrator input voltage and the reference voltage of comparator 1 are both taken from E_s. τ_k is the time which the

monostable multivibrator spends in the quasistable state: $\tau_k \approx 0.7R_{14}C_6$ = 357 microseconds. When the power supply voltage is changing, there may be very small changes in τ_k, but because $T' = R_2C_1 \cdot R_6/R_5$ = 6.667 milliseconds, about 18 times as great as τ_k, the very small change in τ_k has an extremely insignificant effect on the period T. Accordingly we may consider the period T of the sawtooth wave to be relatively constant. The results have proven this point: when the power supply voltage drops from 6.25 V to 5.25 V, there is a change of only 0.14 percent in the period.

B. Stability of the Relationship Between the Measured Parameter and the Pulse Duty Factor

The relationship between the measured parameter and the pulse duty factor is as shown in Figure 5.

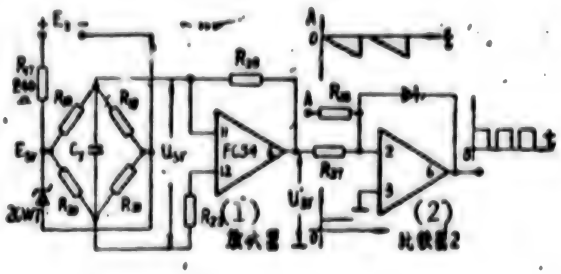

Figure 5.

Key: 1. Amplifier 2. Comparator 2

When the air pressure P is equal to zero, the circuit is at $u_{sr} = u_{sr0}$, $u'_{sr} = \beta u_{sr0} = u'_{sr0}$, and during the period of time t_0 when the monostable multivibrator switches to integrator output $u_a(t) = R_{28}u'_{sr0}/R_{27}$, the output of comparator 2 is low, switching transistor BT5 is off, and there is transmission. During the rest of the time ($T \sim t_0$) because the output of comparator 2 is high, switching transistor BG5 is short circuited and emission stops. Here, the duty factor is determined by whether or not there is transmission during the fixed time period T, and accordingly the pulse duty factor during this period is t_0/T, when the air pressure rises from zero to P_1, P_2, P_3..., u_{sr} rises from u_{sr0} to u_{sr1}, u_{sr2}, u_{sr3} ..., and u'_{sr} changes from βu_{sr0}, βu_{sr1}, βu_{sr2}, βu_{sr3}.... The emission time increases from t_0 to t_1, t_2, t_3.... Accordingly the duty factor increases from t_0/T, t_1/T, t_2/T, t_3/T.... The relationship can be clearly seen in Figure 6.

Because the sawtooth wave increases linearly, $(t_1 - t_0)/T$, $(t_2 - T_1)/T$, $(t_3 - t_2)/T$... and $(u_{sr1} - u_{sr0})$, $(u_{sr2} - u_{sr0})$, $(u_{sr3} - u_{sr0})$... are in a linear relationship, and the relationship between the increase in the emission time and the increase in the measured parameter can be expressed as follows: is $\Delta u_{sr} = \alpha\Delta P$, then

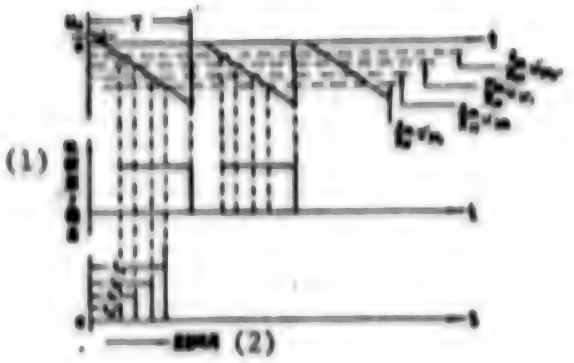

Figure 6.

Key: 1. Comparator 2 output 2. Transmission time

$$t = \frac{T_4 R_{28}}{E_B R_{26}} \beta\alpha\Delta P; \tag{5}$$

where β is the amplifier gain; and α is the conversion factor between the measurement bridge output voltage and the air pressure.

When β and α are constant, the increase in the emission time and the increase in the measured gas pressure are in a linear relationship, so that the increase in the duty factor is in a linear relationship to the increase in the air pressure. The reason that we use the imbalance of the measuring bridge to make the emission time t_0 larger than τ_k when the tire pressure is P_0 is in order to avoid the period of time τ_k and cause the relationship between ΔP and Δt to have excellent linearity throughout. This initial value can be manually set to zero at the receiver output stage so as to cancel it out.

But it can be seen from equation (5) that when the measured parameter is unchanged, when E_B changes, there will be a change in the emission time, and accordingly in the duty factor. Furthermore, because of the change in the battery voltage, if the measured parameter does not change, u_{sr} will change, which will also affect the duty factor. Below we discuss several aspects of its influence.

(1) The effect of changes in E_B if the power supply voltage is changing and u_{sr} does not change. For convenience of discussion, we assume that the measured parameter starts increasing from zero, as does u_{sr}, and that the sawtooth wave is continuous, i.e., that $\tau_k = 0$. In reality, the results will be the same no matter what starting point we use in the discussion. In this case, the emission time t corresponding to any tire pressure value P will show the following relationships:

$$t = \frac{T_1 R_{20}\beta\Delta P}{R_{21}E_s}; \qquad (6)$$

$$\frac{\partial t}{\partial E_s} = \frac{T_1 R_{20}\beta\Delta P}{R_{21}} \cdot \frac{-1}{E_s^2};$$

$$\Delta t \approx \frac{T_1 R_{20}\beta\Delta P}{R_{21}} \cdot \frac{-\Delta E_s}{E_s^2}; \qquad (7)$$

$$\frac{\Delta t}{t} = \frac{-\Delta E_s}{E_s}. \qquad (8)$$

Experience shows that when the apparatus has been operating continuously for 4 hours, the power supply voltage E_1 falls from 6.25 V to 5.95 V and the forward voltage drop at D_1 decreases from 0.617 V to 0.608 V, i.e., E_s falls from 0.617 V to 0.608 V, ΔE_s = 9mV; if we substitute for E_s and ΔE_s in equation (8) we obtain

$$\frac{\Delta t}{t} = \frac{9}{617} = 0.015;$$

i.e. after 4 hours' continuous operation, because the drop in the battery voltage causes a maximum change of 1.5 percent in the emission time corresponding to any measured parameter, the maximum increase in the duty factor is also 1.5 percent.

(2) The effect on the duty factor of a change in u_{sr} resulting from a change in the power supply voltage if the rise rate of the sawtooth wave is constant and the measured parameter is unchanged. R_{20} and R_{21} in Figure 5 are the strain plate resistances of the pressure transducer, with resistance values of 320 ohms. R_{18} and R_{19} are external resistors with values of 3 kilohms. We can see from the diagram that

$$u_{sr} = \frac{\Delta R}{R_{20} + R_{21}} E_{sr}; \qquad (9)$$

where ΔR is the change in the strain plate resistance corresponding to any change in pressure; and E_{sr} is the bridge power supply voltage. The emission time corresponding to any air pressure is

$$t = \frac{T_1 R_{20}\beta}{R_{21}E_s} \cdot \frac{\Delta R}{R_{20} + R_{21}} E_{sr}; \qquad (10)$$

$$\frac{\partial t}{\partial E_{sr}} = \frac{T_1 R_{20}\beta}{R_{21}E_s} \cdot \frac{\Delta R}{R_{20} + R_{21}};$$

$$\Delta t \approx \frac{T_1 R_{20}\beta}{R_{21}E_s} \cdot \frac{\Delta R}{R_{20} R_{21}} \Delta E_{sr}; \qquad (11)$$

$$\frac{\Delta t}{t} = \frac{\Delta E_{sr}}{E_{sr}}. \qquad (12)$$

E_{sr} is supplied through voltage regulator 2CW7, E_w = 3.5 V, $r \leqslant 80$ ohms; this voltage is also specially supplied by a group of cells (E_2 = 6.25 V). Tests confirm that after 4 hours of continuous operation, the battery voltage E_2 drops from 6.25 V to 5.25 V, i.e., a drop of 0.3 V.

Accordingly, $$\Delta E_{gr} \approx \frac{r'}{R_{17} + r'} \Delta E_2;$$

where r' // (R_{20} + R_{21}) // (R_{18} + R_{19}) 70 ohms. (Note: The symbol // indicates parallel connection),

$$R_{17} = 240 \text{ ohms};$$

i.e. $$\Delta E_{gr} = \frac{-2.1}{31} \text{ V};$$

if we substitute E_{gr} and ΔE_{gr} into equation (12) we obtain

$$\frac{\Delta T}{t} = \frac{-2.1}{31 \times 3.5} = 0.019.$$

thus after 4 hours of continuous operation, the drop in E_{gr} causes a decrease of 1.9 percent in emission time (and thus in the maximum change in the duty factor).

(3) The effect of amplifier stability. The amplifier is a high-quality FC54J component, and the closed-loop amplification factor is set at only 50, so that the gain is rather stable. But when the battery voltage changes, its unbalanced output changes. Tests indicate that when the positive and negative potentials both change by 1 V, the amplifier output drift is 0.5 of the maximum output when u_{gr} is a maximum. This value affects the zero point, but to a relatively small degree. Moreover, when the direction of drift is the same as the direction of action of u_{gr}, it has a certain compensating effect on the decrease in u_{gr} resulting from the drop in E_{gr}.

It is apparent that after the apparatus has operated continuously for several hours, and the battery voltage drops, so that E_g falls, the drop results in an increase in the emission time, i.e. the duty factor; on the other hand, E_{gr} drops in accordance with the battery voltage, and this drop results in a decrease in the emission time and hence the duty factor. The two changes exist at the same time and have opposite effects, so that if the battery voltage changes, the effects of the factors which are decisive for the precision of the apparatus are greatly weakened, thus assuring that the apparatus will have relatively high precision. This point has also been proven experimentally.

C. Temperature Stability

Because the receiver is in a constant-temperature control room, and the transmitting equipment is on-site, the temperature primarily affects the transmitter. Here we will not discuss the intrinsic temperature drift of the pressure transducer itself, but will limit ourselves to the temperature stability of the transmitter circuits. It can be seen from the diagram that the temperature effect on the transmitter stems primarily from drops in the reference voltage E_g resulting from temperature changes. Temperature effects on the other sections are quite secondary. Because the reference voltage E_g is obtained from the forward voltage diodes 2CP12, on the basis of the diode forward current formula

$$I_D = I_s(e^{\frac{Vq}{kT}} - 1) \approx I_{se}^{\frac{Vq}{kT}}; \qquad (13)$$

where I_s is the reverse saturation current, $I_s = I_s(T_0)e^{\alpha(T-T_0)}$; T is the absolute temperature in degrees Kelvin; the handbooks state that at constant temperature (25°C), $I_s \leq 5$ microamperes; α 0.13 deg^{-1} K; k is the Boltzmann constant (1.38×10^{-23} J/deg K); q is the charge of the electron (1.602×10^{-19} coulombs); and I_d is the forward current (in this circuit I_d = 2.4 mA).

We can rewrite formula (13) as:

$$V = \frac{kT}{q} \ln \frac{I_D}{I_s} = \frac{kT}{q} \ln \frac{I_D}{I_s(T_0)e^{\alpha(T-T_0)}};$$

$$\frac{\partial V}{\partial T} = \frac{k}{q} \ln \frac{I_D}{I_s(T_0)e^{\alpha(T-T_0)}} - \frac{kT}{q}\cdot\alpha; \qquad (14)$$

Substituting the values given above into equation (14) we obtain

$$\frac{\partial V}{\partial T} = -2.81 \text{ mA/°K}$$

Approximately, for every 1 degree increase in temperature, $\Delta E_g = -2.81$ mV, so that

$$\frac{\Delta E_g}{E_g} = \frac{-2.81}{617} = 0.0046.$$

We can see from the above discussion of the effect of changes in E_g on the precision of our device that every 1 degree C change in the ambient temperature results in an additional error of 0.46 percent. If the ambient temperature change during 4 hours of operation is 10°C, the error will be 4.6 percent, which will seriously affect accuracy. But we must bear in mind that if the change in E_{gr} and the change in E_g are in the same direction, their effects will cancel each other out. If for E_{gr} we use 3 series-connected diode forward power supplies of the same model as E_1 and with similar characteristics, and make their forward currents the same, then when the temperature changes, the two effects will cancel each other out and temperature stability will be preserved.

On the basis of the considerations given above, R_{17} should be taken as 820 ohms, and if E_2 still changes by 0.3 V, then the decrease in E_{gr} will produce a decrease of 1.8 percent in the duty factor. This does not have much effect in compensating the increase in the duty factor resulting from a decrease in E_g.

D. The Excellent Noise Immunity of the Apparatus

As discussed above, one of the main reasons why the precision of AM type remote sensing equipment is not high is that it is rather susceptible to interference, while the main reason that the precision of FM type apparatus is not high is the

nonlinearity of the frequency modulating components. The main point of the approach proposed here is to overcome the main shortcomings of these two methods, obtaining excellent linearity and relatively strong noise immunity. The excellent linearity of this method has already been discussed above, but why does it have excellent noise immunity? The transmitting section of the apparatus uses a 27 MHz crystal oscillator and the receiver uses a 27.464 MHz crystal main oscillator with relatively stable frequency. The superheterodyne reception method is used, and provided that there is no self-oscillation, tuning over the entire frequency band will be rather narrow, assuring very good selectivity and providing sufficiently high gain. When the receiver is less than 10 meters away from the transmitter, a square wave with a peak-to-peak figure of at least 0.5 V can be obtained after detection. Since the measured parameter is related only to the pulse duty factor of transmission, and the last stage of the receiver is also related only to that factor and not to the pulse duration. The circuit between the detector and the discriminator is shown in Figure 7; the waveforms at points A, B, C and D are as shown in Figure 8a, b, c and d. It can be seen that provided the interference signal amplitude after detection is less than 0.25 V, it has no effect on our apparatus. Generally such a large noise-to-signal ratio is rather unlikely, because even if the amplitude of certain high frequency noise (about 27 MH) exceeds this value and causes the discriminator to operate incorrectly, because the demodulator output is reflected in an average value of a sawtooth wave and an additional noise filter stage is added in the buffer stage output, so that the pulse duty factor modulation method (PLM) can yield high noise immunity.

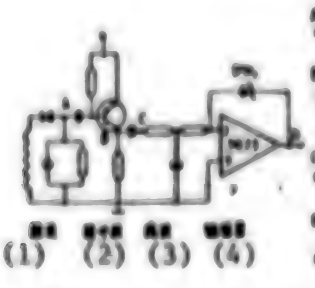

Figure 7.

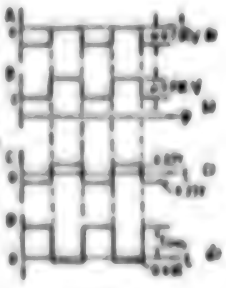

Figure 8.

Key:
1. Detector
2. Buffer stage
3. [illegible]
4. Discriminator

4. Data and Discussion

A. Test Data

Repeated tests and final acceptance testing yielded data which were basically in agreement with those in Table 1. The pressure was read out by a pressure tester, and the output was displayed on a PV-8 digital voltmeter.

It can be seen from the results in Table 1 that our apparatus (including the pressure sensor) had a precision within 1 percent.

Table 1.

(1)	(2) 压力 (公斤/厘米²)										
时间	0	1	2	3	4	5	6	7	8	9	10
	(3) 电流 (安)										
10:00	+0.000	+0.010	+0.020	+0.030	+0.040	+0.050	+0.060	+0.070	+0.080	+0.091	+0.100
11:00	-0.001	+0.009	+0.019	+0.029	+0.039	+0.049	+0.059	+0.069	+0.079	+0.089	+0.099
12:00	-0.000	+0.010	+0.020	+0.030	+0.039	+0.050	+0.060	+0.070	+0.080	+0.090	+0.099
13:00	+0.000	+0.010	+0.020	+0.030	+0.039	+0.049	+0.059	+0.069	+0.079	+0.090	+0.099
14:00	+0.001	+0.011	+0.021	+0.031	+0.041	+0.051	+0.061	+0.071	+0.081	+0.091	+0.101

B. Comparison with similar foreign products using batteries

Table 2. Comparison With Foreign and Domestic Products of Similar Type With Battery Power Supply

Product	Type	Precision	Noise Immunity	Continuous operation before battery change
Apparatus described in this article	PLM	1 percent	Excellent	Over 4 hours
Other domestic products	FM AM-FM	<10 percent	Subject to interference	Unknown
Bolimo [phonetic] Co. TM-10 (Japan)	FM	<10 percent	Subject to interference	Unknown
West Japan Trading Company TM-120 (1975 product)	FM	Receiver linearity <2 percent; no data on overall precision available	Subject to interference	Unknown

The apparatus was designed for remote sensing of parameters which change relatively slowly. To sense parameters which change more rapidly, suitable adjustments must be made in some circuit parameters. Other parameters which change relatively slowly, such as temperature and deformation, can be measured in a similar fashion. If a synchronous electronic distributor is added to both the transmitting and receiving apparatus, the apparatus can measure several parameters simultaneously.

In summary, use of the pulse length modulation method is an effective, high-precision, noise-immune method of remote sensing of certain parameters.

8480
CSO: 8111/0370

BRIEFS

REMOTE SENSING DEVICES--Shanghai, 11 Feb (XINHUA)--The Shanghai Institute of Technical Physics said this week it has developed a multi-spectrum scanner to probe for ore deposits and underground water. It has developed altogether six types of remote sensing devices to help scientists assess the properties, shape, size and degree of movement of objects not easily accessible, like rock strata. The institute has also developed infra-red theremomenters and other contactless type detectors for industry, agriculture, medicine and the fire service. [OW112341 Beijing XINHUA in English 1205 GMT 11 Feb 81]

VIDEO DISPLAY TERMINAL--Beijing, 16 Feb (XINHUA)--China is now producing a versatile video display terminal for use in industry, scientific research and education. Li Shicai, 36, of the signal analysis and processing laboratory of the acoustics institute under the Academy of Sciences, who led the team that developed the terminal, said this week that the VDT is the first of its kind ever made in China and its ability to display diagrams as well as character data makes it particularly useful in industrial design problems. One of its functions, now being further developed by the institute, is the display in diagramatic form of surface vibration on aircraft fuselages. The technology has been bought by a factory and the terminal is now in serial production. [Text] [Beijing XINHUA in English 0735 GMT 16 Feb 81]

CHARACTER COMPUTER--Beijing, 15 Feb (Xinhua)--The Electronic Computer Technology Institute in Beijing recently designed a new computerized Chinese character processing system, BCT-1. It consists of a Chinese character input keyboard, a miniature electronic computer, a computer screen, a typewriter and some software. It can handle about 5,000 frequently used Chinese characters and print about 10 characters per second. The new system will provide an important means for the automation of Chinese press printing and scientific and technological information reference. [OW171115 Beijing Xinhua Domestic Service in Chinese 0010 GMT 15 Feb 81]

CSO: 4008

SOCIAL FORCES USED TO FIGHT MENTAL ILLNESS IN SHANGHAI

Shanghai WEN HUI BAO in Chinese 5 Nov 80 p 2

[Report by Shi Haigen [2457 3189 2704]: "Rely on Social Forces To Do a Good Job of Preventing and Treating Mental Illness; Relapse Rate of Mental Patients in Nanshi Ward Greatly Decreased"]

[Text] Notable results have been obtained from mobilizing and relying on various social forces and from enthusiastically developing the prevention and treatment of mental illness by the leading group for the work in Nanshi Ward. The relapse rate of mental patients has dropped from 29.26 to 8.9 percent.

To strengthen the administration of mental patients and to prevent them from endangering the social order, this ward established a leading group for the prevention and treatment of mental illness, in participation with comrades in charge of departments including those of public health, civil administration, public security, real estate, and collective services bureaus as well as the mental illness hospital in the ward. Neighborhoods established corresponding organs which coordinate with each other to perform well in this task. At present, the ward operates 17 work therapy groups and has taken in 233 mental patients. Section hospitals and 75 large and medium-size factories in the ward have launched the work of prevention and treatment of mental illness. An observation network has been established by 152 resident committees, so that patients can receive treatment nearby and be administered to on the spot; good results have been obtained. According to an analysis of 632 cases at 14 section hospitals, the relapse rate of mental patients dropped from 50.8 to 12.5 percent after the work of preventing and treating mental illness was popularly launched. The social disturbance rate of mental patients declined markedly. According to the statistics of 13 resident committees, it decreased from 3.3 to 1.2 percent and has had a definite effect in alleviating the suffering of patients and reducing concern among staff workers.

9586
CSO: 4008

WORK THERAPY USED TO TREAT MENTAL ILLNESS IN BEIJING

Beijing BEIJING RIBAO in Chinese 6 Jan 81 p 2

[Report by Qin Naijin [4440 6621 3160]: "Mental Illness Prevention and Treatment Clinic in Xuanwu Ward Establishes Work Therapy Station; Patients Organized To Participate in Production and Receive Treatment"]

[Text] The Mental Illness Prevention and Treatment Clinic in Xuanwu Ward has established a work therapy station for mental patients and has organized some of the less serious patients, outpatients, and those who are in their recovery period after hospital discharge to do productive work and receive treatment at the same time. This kind of work therapy not only lightens the burden of patients' families but also contributes to social stability.

In the past, mental patients living at home frequently roamed about in society, endangering their own safety and affecting social stability. In June 1978, the clinic established a work therapy station for mental patients under the support of the ward bureaus of public security and public health. This station combines work, recreation, and pharmaceutical treatment to create a good, normal working and living environment for patients, so they may feel the pleasure of work and joys of life. This helps their recovery of normal thinking and ability to work. Patients participating in work therapy labor for 6 hours a day. During rest periods they take part in recreation activities such as playing chess and cards and listening to radiobroadcasts. Patients usually are organized to watch one or two movies each month and to participate in outings in the spring and fall. Medical personnel also pay attention to their ideological work at all times and resolve problems once detected. After entering the station to receive work therapy, an absolute majority of these patients have been aboe to start and finish work on time, observe labor discipline, and consciously accept the administration of medical personnel. Up to the present, the illness of an absolute majority of the 46 patients receiving work therapy has clearly improved, and 14 of them have basically recovered.

9586
CSO: 4008

PUBLICATIONS

ANNUAL INDEX OF 'YUANZIHE WULI,' 1980

Beijing YUANZIHE WULI [CHINESE JOURNAL OF NUCLEAR PHYSICS] in English Vol 2 No 4, 1980 pp 390-392

[Text]

Sun Hancheng, Yao Jinzhang, Sun Tsuzun, Wen Keling, Lu Huijun, Dai Nengxiong, Jin Ronghua, Yan Chen

D + ^{6}Li and α + ^{6}Li Quasi-Free Processes at Low Energies 1,1(1979)

Zhang Huanqiao, Liu Zuhua

The Measurement of the Average Number of Prompt Neutrons and the Distribution of Prompt Neutron Numbers for ^{252}Cf Spontaneous 1,9(1979)

Zhang Huanqiao, Xu Jincheng, Wen Tongqing

Determination of the Half-Lives of α Disintegration and Spontaneous Fission of ^{244}Cm 1,21(1979)

Chu Yungtai, Fan Guoying, Wu Zhongli, Feng Enpu, Liang Guoshao, Li Fawei, Jiao Dunlong, Li Xianhui, Gao Yingxiang, Xia Guozhong, Su Yinquan, Xiao Qinpian

The Research of Scattering and Transfer Reaction of ^{12}C with ^{12}C 1,31(1979)

Shi Zongren, Shi Xiamin, Zeng Xiantang, Lu Zhirong, Xing Jinqiang, Shen Ronglin, Ding Dazhao

Gamma-Ray Productions Cross Sections from Interactions of 14.9 MeV Neutrons with C, F, Al, Si, Fe and Cu 1,45 (1979)

Wang Xinlin, Wang Shumao, Mao Zhenlin, Wang Fanglin, Ceng Pinlin

Deuteron-Induced Reactions on ^{12}C at Bombarding Energy of 9MeV 1, 63(1979)

Yu Jusheng, Wang Sufang, Tian Yuhong, Hou Mingdong, Miao Degui, Zeng Wenbing, Li Guangwei

Study of the Fission of the Excited Nuclei near Radium 2, 19(1980)

Xu Jincheng, Liu Zuhua, Wen Tongqing, Ding Shengyao, Chen Zhicai

The Dependence of Average Numbers of Prompt Fission Neutron of ^{239}Pu on Incident Fast Neutron Energies 2, 29 (1980)

Yang Chunxiang, Li Guangsheng, Weng Peikun, Cheng Shiping, Liou Fengyeng, Zhou Ling, Zhang Youfang

The Decay of ^{99}Mo 2,41(1980)

Ma Hongchang, Li Jizhou, Huang Jianzhou, Fan Peiguo, Lu Hanlin

Measurement of Cross Section for the Reaction ^{45}Sc (n,2n)^{44}Sc^{m} and Isomeric Cross Section Ratio σ_m/σ_g 2,47(1980)

Liu Zuhua, Zhang Huanqiao

The Distribution of Prompt Neutron Numbers for Long Range-Particle-Accompanied Fission of ^{252}Cf 2, 53(1980)

Yan Chen, Sun Hancheng, Na Xiangyin, Ma Weiyi, Cui Yunfeng, Hu Xuanwen

The Neutron Spectra of ^{7}Li(d,n)Reaction Induced by 400-1020 keV Deuterons 2, 137 (1980)

Ye Binqi, Wen Keling, Zhang Peihua, Yuan Rongfang, Huan Bingyin

Interaction of 9.05MeV Deuteron on ^{7}Li Nucleus 2, 147(1980)

Yang Jinqing, Ni Xinbai, Chang Yingqi, Jiang Dazhen, Cheng Xiaowu

(α,p) Reactions Induced by 31.2 MeV α Particles 2,155(1980)

Huang Jianzhou, Lu Hanlin, Li Jizhou, Fan Peiguo

Excitation Curve Measurement for the Reaction ^{89}Y(n,2n) ^{88}Y 2,213(1980)

Zhang Peihua, Sun Zuhsun, Wen Keling, Wang Fanglin, Wang Shumao

Quasi-Free Scattering in ^{6,7}Li(α,2α)^{1,3}H Reactions at Low Energy 2,219(1980)

Huang Zhengde, Cao Zhong, Li Zhankui, Wu Yongshun, Guo Taichang, Wang Huizhu, Su Qiong, Ding Dazhao

A γ-Ray Spectrometer System for Measurement of Secondary γ-Ray Spectra, Produced in Fast Neutron Reaction 2,229(1980)

Ma Weiyi, Wang Dao, Yan Chen, Sun Hancheng

^{7}Li(d,n) Neutron Spectra and the ^{7}Li (d,2α)n Reaction Induced by 13.2 MeV Deuterons 2,239(1980)

Lu Hanlin, Li Jizhou, Fan Peiguo, Huang Jianzhou

Measurement of Cross Section for the Reaction ^{55}Mn(n,2n)^{54}Mn 2,286(1980)

Li Qingli, Lu Fubao, Han Shukui, Guo Qingjiang, Li Zhichang, Chen Ruixie, Dong Zhijia, Jiang Chenglie

Intermediate Resonances in the Region of Deutron Energy from 1.0 to 2.5 MeV in the ^{28}Si(d,p)^{29}Si Reaction 2,316 (1980)

Bai Xixiang, Wen Shenlin, Sun Daze, Li Anli, Chen Guanren, Huang Tangzi, Sun Fengxian

The Angular Distribution for Elastic Scattering of 14.7 MeV Neutrons by Deuterons and the Neutron Spectra from the Break-up of Deuterons 2,327(1980)

Fan Peiguo, Lu Hanlin, Li Jizhou, Huang Jianzhou

The Broad Structure in the Excitation Curve of ^{115}In(n,n')^{115m}In Reaction 2,337(1980)

Luo Yixiao, Liang Zongli, Xiao Jianmin, Guo Junsheng

The Transport Characteristics of Gas-Jet Recoil Transport System and the Application to the Transport of Reaction Products Produced by Fast Neutron 2,343 (1980)

Chao Zhong

Timing of Low Energy Charged Particles by Si (Au) Detector and its Application in a Time of Flight Spectrometer 2,376(1980)

Chen Shiping, Liu Fengying, Zhou Ling, Yang Chunxiang, Li Guangsheng, Weng Peikun, Zhang youjang

γ-Ray Spectrum from ^{147}Nd Decay 2,382 (1980)

Li Zhuxia, Zhang Xizhen, Su Benhao, Shi Yijin

The Effects of Core Polarization on the Single Particle State in ^{208}Pb 1, 73(1979)

Su Zongdi, Zhang Jingshang, Shi Xiangjun, Wang Shunuan, Tang Xuetian, Tian Ye, Wang Cuilan

The Statistical Theory of Nuclear Reactions and its Application to Fissionable Nuclei 1,81(1979)

Wang Shunuan

Calculation of Half-Lives of Fission Isomers 1, 129(1979)

Zhang Jingshang, Zhuo Yizhong, Gu YingQi

The Transport Process of the Coupling System Between the Single Particle and the Phonon 2,1(1980)

Zhang Xizhen, Ma Zongyu

The Treatment of Spurious States in Nuclear Field Theory 2,11(1980)

Zhang Xizhen, Su Benhao, Ma Zhongyu

Renormalization of Double Phonon State 2,84 (1980)

Su Benhao, Shi Tijin, Zhang Xizhen, Su Zongdi

A Coupling Dyson Equation by Considering the Meson Degree of Freedom in Nuclei 2,87(1980)

Chu Lianyuan

The Theory of (n,2n) Reaction for Light Nuclei 2, 91 (1980)

S.S.M.Wong, Su Banhao, Su Zongdi, Lu Zongdao, Chang Hzichen

A Preliminary Study of the Mass Distributions in Deep Inelastic Scattering of Heavy Ions 2,97(1980)

J.O.Rasmussen, Ma Zhongyu, Wu Xizhen, Zhang Jingshang, Zhuo Yizhong, Wang Yanzen, Qiu Zhihong, Yang Fujia

Calculation of Muon State Probabilities after Muon-Induced Fission 2,107(1980)

Xu Gongou

A Kind of Formulation of Quantum Statistical Mechanics 2,115(1980)

Han Wenshu, Zhuang Fei

The Final State Interactions in d+^{6}Li Three-Body Reactions 2, 123(1980)

Chen Baoqiu

On ^{6}Li(p,pd)α and ^{6}Li (d,2d)α analysis of Quasifree Scattering 2, 131(1980)

Shi Yijin, Han Wenshu, Lu Zhaoqi, Zheng Yuming

The Formulae of Overlapping Integral, Kinetic and Potential Energy of Many-Well Shell Model for Arbitrary Cluster-Partition 2,166(1980)

Yu Zurong

Application of the Resonance Group Method in the Quark-Cluster Model 2,189(18980)

Wu Shishu, Yao Yujie

Muitiple Scattering Formalism and Method

of Green's Functions 2,193(1980)

Zeng Jinyan, Yang Fuchia

The $Z^{-1/3}$-Law for the Nuclear Giant Resonance Energy 2,245(1980)

Zhang Xizhen, He Hanxing, Chen Yongzhou, Gao Yuanyi

Backbending Mechanism of ^{166,168}Er 2,253(1980)

Wu Xizhen, Zhao Yizhong

Brownian Motion and Fission Rate 2,257 (1980)

Wang Fan, He Yin

Quark Force and Nuclear Force I. n-p Scattering 2,261(1980)

He Yin, Zheng Yuming, Lu Zhaoqi, Wang Fan

Quark Force and Nuclear Force II. Comparing with the Phenomenological Nuclear Force 2,289(1980)

Zhang Xizhen, Zhang Jingye

Systematics of Aligned Angular Momentum for Even-Even Nuclei in Rare-Earth Region 2,297(1980)

Zhang Qingying

The Formulas of the Matrix Elements of the Noncentral Forces 2,302(1980)

He Yukun, Pan Chenying

A Variational Perturbation Method for the Calculation of Neutron Induced γ-Ray Spectra 2,307 (1980)

Sun Xiangfu, Pan Zongyou, Yuan Shuanggui, Xu Guojun

Determination of the Lifetime of Excited Compound Nuclei from $^{12}C+^{197}Au$ Reaction by Blocking Effect 1,93(1980)

Zhang Guenlin, Hu Wenxiang, Zhou Weiguan

Determination of Mössbauer Parameters from Unresolved Spectra 2,59 (1980)

Institute of Atomic Energy, Daqing Oilfield Research and Planning Institute Field Experience to Verify Principle of Ge(Li)-$(n,n'\gamma)$ Gamma Ray Spectrometry Well Logging(Research Notes)2,160(1980); (Article)2,277(1980)

Guo Shilun, Zhou Shuhua, Meng Wu, Zhang Pengfa, Sun Shengfen, Hao Xiuhong, Liu Shunzheng, Zhang Feng, Hu Ruiying, Liu Jingfa

Age Determination of Beijing Man(Peking Man) by Fission Track Dating 2,183(1980)

B.J. Deutch, C.H. Liu, Lu Fuquan, Sun Changnian, Tang Jiayong, Tang Guohun, Xu Keshou, Yang Fujia, Ye Hui

Nuclear Polarization of ^{13}N Via Ion Beam-Foil Interaction 2,205(1980)

G.M. Temmer

Lepton Channeling and Radiation Properties in Crystals 2,353(1980)

J. Siejka, Chen Huansheng

Determination of the Total Amount of Oxygen Atoms in Silicon Oxide Surface Layers by the Nuclear Reaction $^{16}O(d,p_1)^{17}O^*$ 2,364 (1980)

Chen Wuzhong

The Isochronous Orbits and Linear Properties in Separated Sector Cyclotron with Practical Field 1, 101 (1979)

Chen Yinbao, Xie Xi

The Nonuniform-Density Space Charge Effect in the Waveguide of Electron Linac 1,107(1979)

Cao Qingxi, Guan Xialing

Dynamics of Particles in a Six-Dimensional Phase Space 2,67(1980)

Guan Xialing, Cao Qingxi

The Beam Optics Method for Designing a Tandem Buncher System 2, 167(1980)

Yu Qingchang

Theory of Transfer Matrices for Intense Ion Beam 2,271(1980)

Chen Yinbao, Xie Xi

Non-Statistical and Statistical 6-Dimensional Phase Space Equations and Their Duality Theorem in Accelerator Beam Transport 2,369(1980)

Li Zhongzhen, Liang Chunxin

The Measurements of the Starting Potential and the Gas Gain of G-M Counters 2, 77 (1980)

Li Zhongzhen, Peng Huazhou

A Further Study of Gas Gain of Multiwire Proportional Chamber 2, 161, (1980)

Fang Jinqing

Simple Solutions of the One-Dimension Plasma-Sheath Equation in Low-Pressure Gas Discharge 2,175(1980)

CSO: 4008

PUBLICATIONS

ANNUAL INDEX OF 'TIANWEN XUEBAO,' 1980

Beijing TIANWEN XUEBAO [ACTA ASTRONOMICA SINICA] in English Vol 21 No 4, 1980 pp iii-iv

[Text]

PLANETS

CELESTIAL MECHANICS

ASTROMETRY

CSO: 4008

PUBLICATIONS

ANNUAL INDEX OF 'QINGHUA DAXUE XUEBAO,' 1980

Beijing QINGHUA DAXUE XUEBAO [JOURNAL OF QINGHUA UNIVERSITY] in English
Vol 20 No 4, 1980 pp 112-114

[Text]

(The figures in the brackets are the Vol. No and Page respectively)

CORRESPONDENCE,

CSO: 4008

PUBLICATIONS

TABLE OF CONTENTS OF 'XI'AN JIAOTONG DAXUE XUEBAO' NO 3, 1980

Xi'an XI'AN JIAOTONG DAXUE XUEBAO [JOURNAL OF XI'AN JIAOTONG UNIVERSITY] in Chinese Vol 14 No 3, Sep 80

9717
CSO: 4008

PUBLICATIONS

TABLE OF CONTENTS OF 'DONGWU XUEBAO' NO 4, 1980

Beijing DONGWU XUEBAO [ACTA ZOOLOGICA SINICA] in Chinese No 4, Dec 80 p 288

Scientific Notes

9717
CSO: 4008

AUTHOR: GUO Changlin [6753 1603 7207]

ORG: Shanghai Institute of Ceramics, Chinese Academy of Sciences

TITLE: "Formation Mechanism and Stereographic Projection Analysis of Growth Ridges on the Surface of the Crystal Grown by the Pulling Method"

SOURCE: Beijing GUISUANYAN XUEBAO [JOURNAL OF THE CHINESE SILICATE SOCIETY] in Chinese No 4, Dec 80 pp 325-338

TEXT OF ENGLISH ABSTRACT: The formation mechanism of the growth ridges on the surface of the crystal grown by the pulling method is described. As the orientation of crystal growth enables the crystal grown under uniform environment to assume certain characteristic shapes (habits) and to present certain exposing planes, the growth ridges and faces on the surface of the crystal grown by the pulling method are naturally the results of the extension of the principal exposing planes under certain growing conditions. The crystallographic conditions under which the ridges are grown on different parts of the crystal surface are described. The method of stereographic projection analysis for deducing the configuration and distribution of growing ridges along different pulling directions is also presented. The deduced configurations of growth ridges on a number of crystals, such as SBN, BNN, BG, Si, LN, LT, etc., have been compared with those obtained from the actual growth of the ridges, and this proves that the method presented is generally applicable and satisfactory.

AUTHOR: ZHANG Fukang [1728 4395 1660]
ZHANG Zhigang [1728 1807 0474]

ORG: Both of the Shanghai Institute of Ceramics, Chinese Academy of Sciences

TITLE: "Ancient Chinese Overglaze Colors"

SOURCE: Beijing GUISUANYAN XUEBAO [JOURNAL OF THE CHINESE SILICATE SOCIETY] in Chinese No 4, Dec 80 pp 339-350

TEXT OF ENGLISH ABSTRACT: With the help of spectro-chemical analysis and the information from the related literature, the authors made a systematic study on ancient Chinese overglaze colors. Based on the chemical compositions obtained, it was found that:
(1) The traditional overglaze colors had their origin in ancient Chinese low-temperature colored glazes. These two different types of decoration used the same and limited number of coloring elements (i.e., iron, copper, cobalt and manganese) to produce a series of brilliant colors. The difference between the low-temperature colored glazes and the overglaze colors lies in the fact that the former belongs to the binary system $PbO-SiO_2$ while the latter belongs to the ternary system $PbO-SiO_2-K_2O$.
(2) The enamel colors imported during the last years of Emperor Kongxi exerted a profound influence on the traditional Chinese overglaze colors, especially the use of arsenic which led to the invention of powder colors.

[Continuation of GUISUANYAN XUEBAO No 4, Dec 80 pp 339-350]

Based on the information from the literature and the conventional techniques still being used at Jingdezhen (Chin Teh Chen), the authors have proposed a method of preparing the ancient Chinese overglaze colors.

AUTHOR: WEN Tinglian [3306 1694 8834]
LI Wenlan [2621 2429 5695]
LI Shichun [2621 0013 2797]

ORG: All of Shanghai Institute of Ceramics, Chinese Academy of Sciences

TITLE: "BN Prepared by Chemical Vapor Deposition"

SOURCE: Beijing GUISUANYAN XUEBAO [JOURNAL OF THE CHINESE SILICATE SOCIETY] in Chinese No 4, Dec 80 pp 351-356

TEXT OF ENGLISH ABSTRACT: CVD BN ceramics have been prepared by using BCl_3 and NH_3 as gaseous raw materials. The effects of temperature, pressure and the ratio of the reactant gases are investigated with the CVD apparatus made at the institute. The optimum deposition conditions for the CVD BN are discussed.

X-ray diffraction and microscopic observation of the CVD BN samples show that the polycrystalline CVD BN produced is isotropic and is composed of radial "ball crystals" formed from fibrous crystallites. The crystal structure of CVD BN has the characteristics of a disordered layer.

AUTHOR: TENG Qin [3326 3830]
NI Peiwen [0242 3099 2429]
ZHANG Yinghua [1728 5391 5478]

ORG: All of the Shanghai Institute of Ceramics, Chinese Academy of Sciences

TITLE: "An Investigation on Control of Refractive Index Profiles for Graded Optical Fiber in the P_2O_5-SiO_2 System"

SOURCE: Beijing GUISUANYAN XUEBAO [JOURNAL OF THE CHINESE SILICATE SOCIETY] in Chinese No 4, Dec 80 pp 357-364

TEXT OF ENGLISH ABSTRACT: A deposition technique program was initially designed to fabricate graded optical fibers in the system P_2O_5-SiO_2 with refractive index profile of $\alpha \approx 2$, based on the waveguide structure of minimum dispersion as suggested by D. Gloge. Experiments resulted in the modification of the program, and a refractive index profile of $\alpha = 1.95 \pm 0.1$ was obtained. Various technological parameters affecting the refractive index are discussed.

AUTHOR: DING Shuxiu [0002 2885 0208]

ORG: Cement Division, Research Institute of Building Materials

TITLE: "Oil-Well Expansive Cement Hardened under Hydrothermal Conditions"

SOURCE: Beijing GUISUANYAN XUEBAO [JOURNAL OF THE CHINESE SILICATE SOCIETY] in Chinese No 4, Dec 80 pp 365-375

TEXT OF ENGLISH ABSTRACT: An oil-well expansive cement containing an appropriate mixture of normal oil-well cement, alumina cement, gypsum and bentonite was cured under various hydrothermal conditions and the mechanical, expansive and water permeability properties thereof were investigated. From phase analysis it has been ascertained that the formation of monosulfo-aluminate hydrate was accelerated by increasing the temperature and by prolonging the curing time. The mechanism of expansion of the cement was also discussed in the paper.

AUTHOR: ZHOU Wenbin [0719 2429 1755]

ORG: Research Institute of Synthetic Crystals, Ministry of Building Materials

TITLE: "Synthesis and Properties of Water-Swelling Fluoromicas and Fluoromontmorillonoids"

SOURCE: Beijing GUISUANYAN XUEBAO [JOURNAL OF THE CHINESE SILICATE SOCIETY] in Chinese No 4, Dec 80 pp 376-384

TEXT OF ENGLISH ABSTRACT: The synthesis and properties of water-swelling fluoromicas are described. The (001)-spacing as determined by X-ray photography increased from 9.5 Å to 14.98 Å, which indicates that two water molecular layers have been adsorbed. Experiments on the sorption of the positive ions and the selective sorption of mixed ions were carried out in an aqueous solution. A simulated test and actual test were made under static conditions with low-level and low intermediate level radioactive wastes respectively. The results lead to the conclusion that the water-swelling fluoromicas have a satisfactory sorption for Cs^{+}, Sr^{2+} as well as for neuclides, such as Cs^{137}, Sr^{89}, Ru^{106}, etc., and therefore are good sorbents.

AUTHOR: XIAO Chaoliang [5135 6389 0081]
BI Jianqing [3968 1696 3237]
WANG Changqing [3769 2490 1987]
CHEN Liquan [7115 4539 3123]

ORG: All of the Institute of Physics, Chinese Academy of Sciences

TITLE: "The Single Crystal Growth of Lisicon Lithium Zinc Germanate by means of the Czochralski Method"

SOURCE: Beijing GUISUANYAN XUEBAO [JOURNAL OF THE CHINESE SILICATE SOCIETY] in Chinese No 4, Dec 80 pp 385-387

TEXT OF ENGLISH ABSTRACT: The single crystals of the Lisicon lithium zinc germanate have been grown by means of the Czochralski method. The influence of the composition of the starting material, constitutional supercooling, etc., on the crystal quality has been investigated. Transparent single crystals free from crevice and cloud with 9~15 mm in diameter and 20 mm in length have been successfully grown under optimum growth conditions.

AUTHOR: GAN Fuxi [1626 4395 3588]

ORG: Shanghai Institute of Optics and Fine Mechanics, Chinese Academy of Sciences

TITLE: "Laser Material Research in China"

SOURCE: Beijing GUISUANYAN XUEBAO [JOURNAL OF THE CHINESE SILICATE SOCIETY] in Chinese No 4, Dec 80 pp 388-396

TEXT OF ENGLISH ABSTRACT: A review of the current status of the development of laser material in China was presented. Emphasis was given to laser glasses, laser crystals and nonlinear optical crystals.

In the early 1960's, laser output was obtained from Nd-doped silicate, borate, phosphate, and fluorophosphate glasses. Great efforts have been made to develop the technological process for making laser glasses with high optical quality and large size. Spectral and luminescent properties of rare earth ions in inorganic were investigated. Detailed studies on the energy transfer process of Nd^{3+} doped laser glasses were developed. Nonlinear optical effects based on the intense laser interaction with the glass medium were described and analyzed.

Over 20 kinds of laser crystals have been grown in China since 1961. The laser performances of ruby, YAG, NdPP and other crystals with different growth techniques have been shown. Extensive study on the various defects in laser crystals,

[Continuation of GUISUANYAN XUEBAO No 4, Dec 80 pp 388-396]

such as facet, twin, inclusion and dislocation, was carried out in China. Some experiments on laser crystal physics were also conducted.

Up to this date, large crystals of KDP, ADP, $LiNbO_3$, BNN, etc., can be grown. More emphasis is laid on the theoretical and technical research for new nonlinear crystals.

AUTHOR: CHEN Zhaoyou [7115 5128 0645]

ORG: Luoyang Refractory Material Research Institute, Ministry of Metallurgical Industry

TITLE: "The Corrosion of Basic Oxygen Furnace (BOF) Linings by Slags"

SOURCE: Beijing GUISUANYAN XUEBAO [JOURNAL OF THE CHINESE SILICATE SOCIETY] in Chinese No 4, Dec 80 pp 397-408

TEXT OF ENGLISH ABSTRACT: This paper presents a survey of the corrosion and mechanism of slag attack on carbon-bearing basic refractories (BOF linings). It is discussed in four parts: (a) oxidation of carbon in BOF linings; (b) slag penetration into the brick pores and measures of prevention; (c) influence of impurity content in refractories and composition of slag on the corrosion of BOF linings; (d) dissolution of the basic refractories in slags and use of dolomite as part of the flux. Finally, some proposals for further research are suggested.

AUTHOR: LI Zhonghe [2621 0022 0735]
WENG Zhenpei [5040 5271 1014]
WU Shugao [7135 2885 4108]

ORG: All of the Shanghai University of Science and Technology

TITLE: "The Crystal Habit and the Characteristic Optical Properties of Barium Titanate Crystal"

SOURCE: Beijing GUISUANYAN XUEBAO [JOURNAL OF THE CHINESE SILICATE SOCIETY] in Chinese No 4, Dec 80 pp 409-413

TEXT OF ENGLISH ABSTRACT: The crystal habit and the characteristic optical properties of barium titanate and the microstructure of barium titanate procelain were investigated.

Barium titanate crystal belongs to the orthorhombic system. Its space group is Pmmn. Its crystal habit is relatively simple. Based on the observation, the three ideal crystal forms are restored. The main simple crystal form which appeared contains orthor-prismatic and parallel two planes. Due to {110} being emphasized, prismatic crystal will be shown.

The optical properties of barium titanate crystal were determined by using super thin, smooth sections of 18 μm thick, and 618 epoxy resin with an index of

[Continuation of GUISUANYAN XUEBAO No 4, Dec 80 pp 409-413]

refraction of 1.5699 was used as the adhesive.

Barium titanate is transparent and colorless, usually euhedral or semi-euhedral with positive high relief and two directions of cleavage, {100} being perfect and {001} medium, strong birefringence, and the maximum interference color can be as high as third-order medium; parallel extinction; sign of elongation either positive or negative; biaxial positive, $2V = 42^{\circ}$, $v > r$; optical orientation: $N_g \parallel a$, $N_m \parallel c$, $N_p \parallel b$.

The barium titanate porcelain has prismatic magniphyric or granulitic microstructures.

AUTHOR: ZHOU Heping [0719 0735 1627]

ORG: Department of Chemistry and Chemical Engineering, Qinghua University

TITLE: "Introduction to the Method of Quantitative Determination of Phase Content of Si_3N_4 by X-ray Diffraction Analysis"

SOURCE: Beijing GUISUANYAN XUEBAO [JOURNAL OF THE CHINESE SILICATE SOCIETY] in Chinese No 4, Dec 80 pp 414-424

TEXT OF ENGLISH ABSTRACT: The basic principle of "normalized method" as reported by P. Gazzara and R. Messier is described briefly. A simple and direct calculation method has been used in the determination of the phase content of Si_3N_4 by using theoretical intensities. Experimental results showed that the method can minimize the effects of the seriously preferred orientation of alpha silicon nitride. The accuracy and reproducibility have been discussed in the article. In order to increase the accuracy of the "normalized method," the importance of reasonable selection of the diffraction peaks of space distribution is stressed. The theoretical intensity values of (111) and (220) diffraction peaks for silicon have been accurately corrected.

AUTHOR: GUAN Jianshi [7070 1696 6684]

ORG: Chongqing Institute of Architectural Engineering

TITLE: "The Activity of Coal Cinder"

SOURCE: Beijing GUISUANYAN XUEBAO [JOURNAL OF THE CHINESE SILICATE SOCIETY] in Chinese No 4, Dec 80 pp 425-429

TEXT OF ENGLISH ABSTRACT: The activity of fuel ash was studied in the light of the original composition of the coal, the burning temperature and the physical-chemical change during the heating process. The author proposes that there exists two temperature ranges in which the ash exhibits activity--the middle and high temperature activity ranges. The key factor of the activity of cinder lies in the decomposition, vitrification and melting of the clay minerals, while the other minerals exhibit almost no effect. When the burning temperature of coal is below 1000°C, the activity of the cinder is produced by the amorphous matter resulting from the decomposition of the clay minerals. If the essential ingredient of the clay minerals is kaolinite, the cinder derives its activity from the metakaolinite. When the burning temperature is over 1200°C, the cinder owes its activity to the vitrified substance.

9717
CSO: 4009

END

END OF FICHE DATE FILMED

9 March 1981